Role of Substrate Defects on the Reverse Leakage Behavior of Vertical GaN Devices

Y. Wang[1*], M.E. Liao[1], K. Huynh[1], W. Olsen[1], X. Huang[2], M. Wojcik[2], J.C. Gallagher[3], T.J. Anderson[3], M.S. Goorsky[1]

[1]University of California Los Angeles, Los Angeles, California, 90095, USA
[2]Advanced Photon Source, Argonne National Laboratory, Argonne, Illinois, 60439, USA
[3] Naval Research Laboratory, Washington, DC 20375, USA
[*]email: zjjxwyk@ucla.edu, Phone: +1 310-913-7669

Keywords: X-ray topography, Gallium Nitride, Reverse Leakage

Abstract

The impacts of the substrate defect on the reverse leakage behavior of vertical GaN p-i-n diodes are investigated. The devices are fabricated on HVPE GaN substrates with periodically patterned dot-cores. where the defect density is higher, and the lattice distortions are larger than the regions in between cores. X-ray topography is employed to image the defect characteristics and the lattice distortion underneath different devices. The distances from each device to the nearest core center can be measured, which is further correlated to the device reverse leakage current from the I-V measurements. It is found that the devices further away from the core centers show substantially lower reverse leakage current, compared to the devices close to the core centers.

Introduction

Vertical GaN power devices are promising candidates for next-generation high power applications. To reduce the threading dislocation density in the HVPE GaN substrates, growth techniques have been demonstrated to produce freestanding GaN substrates with periodically positioned inversion domains known as "cores", with an average spacing of ~1 mm [1, 2]. Earlier studies have shown that threading dislocations are direct causes for reverse leakage current in both heteroepitaxial [3, 4] and homoepitaxial GaN-based devices [5]. However, comparisons were usually made between devices fabricated separately on different wafers. Meanwhile, a general assumption made is that the defect distribution is uniform and the device leakage current at the measured location on the wafer is representative of the whole sample. However, the assumption may not hold for substrate with non-uniform defect distribution (such as the dot-core substrate), where defect density at different locations on the wafer can vary up to a few orders of magnitude. In this study, we compare the reverse leakage current from vertical GaN devices fabricated in the same run but located on different positions on a wafer. Taking advantage of the inhomogeneous but very predictable defect distribution in the dot-core GaN substrate, the impact of the substrate defect density on the reverse leakage behavior of vertical GaN devices can be understood.

Samples and Experimental Methods

The structure of the p-i-n diodes fabricated on dot-core HVPE GaN substrates is shown in figure 1a. Each structure consisted of an 8 μm MOCVD n-type (10^{16} cm^{-3}) layer followed by a p-GaN layer of 500 nm [Mg]>10^{19} cm^{-3} and a 15 nm capping layer with [Mg]>10^{20} cm^{-3}. The details of the fabrication process have been reported earlier by Gallagher et al [6]. Current-voltage (I-V) measurements were taken using a Keithley 4200 analyzer with a preamplifier. The triple axis X-ray measurements used a Bruker D1, with an incident beam mirror to produce a parallel beam (Cu kα1 radiation) and a Si (220) channel cut collimator. The scattered beam optics included a Si (220) channel cut crystal. Synchrotron double crystal x-ray topography measurements, with a Si (333) first crystal as a beam expander, were performed at the 1-BM Beamline of the Advanced Photon Source, Argonne National Laboratory with a photon energy of 8.05 keV with the GaN ($11\bar{2}4$) reflection. A schematic with the experimental setup is shown in figure 1b.

Results and Discussion

A major characteristic of the dot-core HVPE substrate is the inhomogeneous defect distribution. To assess the variation, triple axis X-ray rocking curve measurements of the GaN (0004) peak were performed at different locations on the wafer. Figure 2 shows representative scans from a region close to a core center and another region away from a core center. The FWHM and the FW0.01M from the region close to the core center are 31 arcsecs and 185 arcsecs. In comparison, the FWHM and the FW0.01M from the region away from the core center are 21 arcsecs and 87 arcsecs. The difference in peak widths results from the difference in dislocation density. An earlier study has shown that regions

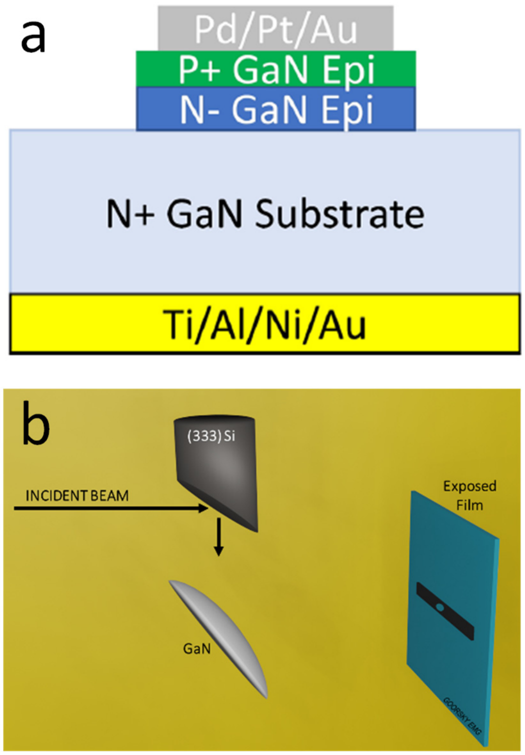

Figure 1. a) the structure of the p-i-n diode used in this study, b) a schematic showing the setup of the synchrotron double crystal x-ray topography measurement.

near the core center have a dislocation density up to 10^8 cm^{-2} while the regions in between cores show dislocation density on the order of 10^4 cm^{-2} [7]. The high dislocation density at the core centers induces large lattice distortions and increased the rocking curve width. Figure 3a shows the x-ray topography image of the wafer. The circles in figure 3a highlight the position of the dot-cores. The spacing of the adjacent cores is ~0.8 mm in a square array. The core regions have large lattice distortions, due to the high dislocation density, and do not diffract with the rest materials. Figure 3b shows the optical microscope image from the same location as the topography image. The device outlines are captured in the topography image, which allows the defect characteristics under each device to be studied separately. The distance of each device from the nearest core centers can also be determined. This is necessary to understand the impacts of the defects on the device leakage behavior.

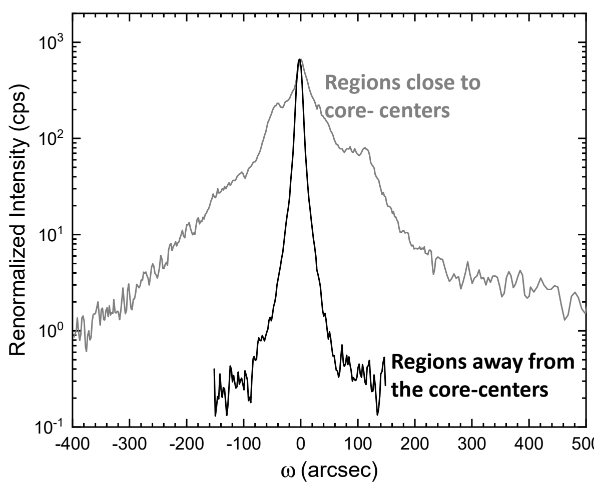

Figure 2. (0004) TAD GaN rocking curves from regions close to core-centers and regions away from the core-centers.

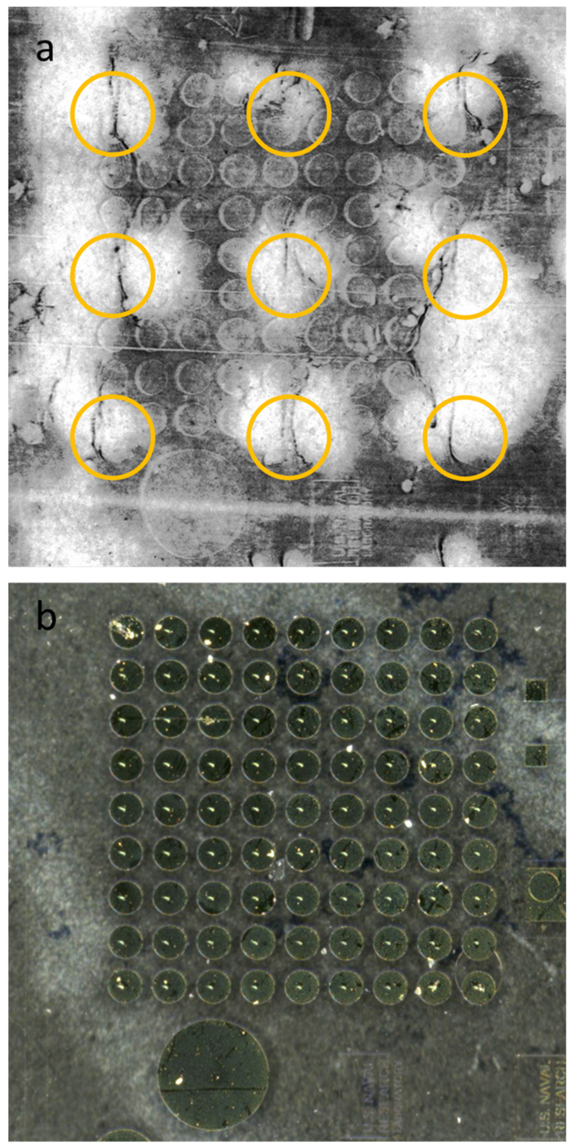

Figure 3. a) x-ray topography image, the circles are the showing the position of cores with large lattice distortions. b) the optical microscope image from the same location on the wafer.

I-V measurements were performed to investigate the reverse leakage current variation from different devices. Figure 4 shows the reverse leakage current at -200V from 8 p-i-n diodes and is plotted with their relative distance to the nearest core center. Among the eight devices, the two devices (Device 2, 8) that are relatively closer to core-centers showed the highest leakage current, above 0.01A/cm^2 at -200V. Overall, as the device gets further away from the core centers, the leakage current decreases. The lowest leakage current at -200 V is just below 10^{-8} A/cm^2, which is over six orders of magnitude lower than the device with the highest leakage current.

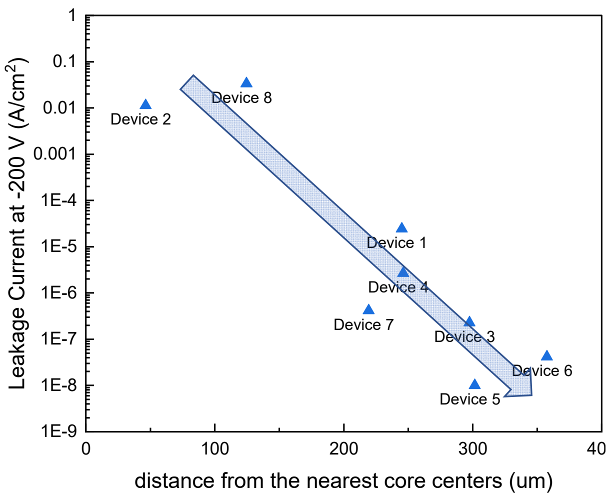

Figure 4. The reverse leakage current at -200V from eight of the p-i-n diodes fabricated on a dot-core GaN substrate plotted with their relative distance to the nearest core-center.

CONCLUSIONS

The relationship between the reverse leakage behavior of GaN based vertical devices and the defect characteristics of the dot-core HVPE GaN substrates was investigated in this work. Triple axis x-ray rocking curves showed a large variation in the peak width on and off the cores. X-ray topography imaged the defective regions under different devices within the same wafer, showing periodic defective regions around the core centers with a high defect density, and high-quality regions in between cores with a low defect density. Taking advantage of the non-uniform but predictable defect distribution of the dot-core substrate, the impact of defects density on the performance of devices with otherwise identical structures can be understood. The p-i-n diodes fabricated on dot-core GaN substrate showed a large variation in the reverse leakage current. Positioning the devices away from the core-centers results in a reduction in the reverse bias leakage by over six orders of magnitude at -200V. The results from this study show that the substrate defect density and distribution play an important role in the device leakage current and x-ray topography is an effective method for studying defect characteristics in the substrate and epi-layer underneath individual devices.

ACKNOWLEDGMENTS

This research was supported through the ARPA-E PNDIODES program under contract DE-AR0001116 at UCLA. This research used resources of the Advanced Photon Source, a U.S. Department of Energy (DOE) Office of Science User Facility operated for the DOE Office of Science by Argonne National Laboratory under contract DE-AC02-06CH11357. The electrical measurements were performed at the U.S. Naval Research Laboratory, supported by the Office of Naval Research.

REFERENCES

1. K. Motoki, T. Okahisa, S. Nakahata, N. Matsumoto, H. Kimura, H. Kasai, K. Takemoto, K. Uematsu, M. Ueno, Y. Kumagai, A. Koukitu, and H. Seki, J. Cryst Growth, **912**, 237-239 (2002).
2. K. Motoki, T. Okahisa, R. Hirota, S. Nakahata, K. Uematsu, and N. Matsumoto, J. Cryst Growth **305**, 377 (2007).
3. Y.-Y. Wong, E.Y. Chang, T.-H. Yang, J.-R. Chang, J.-T. Ku, M.K. Hudait, W.-C. Chou, M. Chen, and K.-L. Lin, J. Electrochem. Soc. **157**, H746 (2010).
4. D. S. Li, H. Chen, H. B. Yu, H. Q. Jia, Q. Huang, and J. M. Zhou, J. Appl. Phys. **96**, 1111 (2004).
5. S. Usami, Y. Ando, A. Tanaka, K. Nagamatsu, M. Deki, M. Kushimoto, S. Nitta, Y. Honda, H. Amano, Y. Sugawara, Y.-Z. Yao, and Y. Ishikawa, Appl. Phys. Lett. **112**, 182106 (2018).
6. J.C. Gallagher, T.J. Anderson, A.D. Koehler, M.A. Ebrish, G.M. Foster, M.A. Mastro, J.K. Hite, B.P. Gunning, R.J. Kaplar, K.D. Hobart and Francis J. Kub, Journal of Electronic Materials, **50** 3013–3021 (2021).
7. T. Nakamura, and K. Motoki, Proc. IEEE., **101**, 2221 (2013).

ACRONYMS

GaN: Gallium Nitride
HVPE: Hydride Vapor Pressure Epitaxy
MOCVD: Metal-Organic Chemical Vapor Deposition
FWHM: Full Width at Half Maximum
FW0.01M: Full Width at 0.01 Maximum